

Project: IEEE P802.15 Working Group for Wireless Personal Area Networks (WPANs)

Submission Title: Measurements and Modeling of THz Chip-to-Chip Channels in Metal Enclosure

Date Submitted: 14 July 2019

Source: Jinbang Fu, Prateek Juyal, and Alenka Zajic

Company: Georgia Institute of Technology

Address: 85 5th Street NW, Atlanta GA 30308

Voice: 404 395-6604, FAX: N/A, E-Mail: alenka.zajic@ece.gatech.edu

Re: n/a

Abstract: In this talk, we will present characterization of Terahertz (THz) wireless channel inside a desktop size metal enclosure as well as statistical modeling of this environment. Measurements indicate that both traveling wave and resonating modes exist inside the metal enclosure. Measurements for line-of-sight (LoS) propagation inside the empty metal enclosure show that the path loss significantly changes as a function of the transceiver's height. It is found that this variation is due the resonant modes contribution in the received power. Furthermore, the path loss model that captures signal strength variation in a resonant cavity is proposed. Finally, it was shown that statistical model can capture propagation in metal enclosures. The results show a good agreement between the simulated and measured statistics.

Purpose: Information of IEEE 802.15 IG THz

Notice: This document has been prepared to assist the IEEE P802.15. It is offered as a basis for discussion and is not binding on the contributing individual(s) or organization(s). The material in this document is subject to change in form and content after further study. The contributor(s) reserve(s) the right to add, amend or withdraw material contained herein.

Release: The contributor acknowledges and accepts that this contribution becomes the property of IEEE and may be made publicly available by P802.15.

Measurements and Modeling of THz Chip-to-Chip Channels in Metal Enclosures

Prof. Alenka Zajić

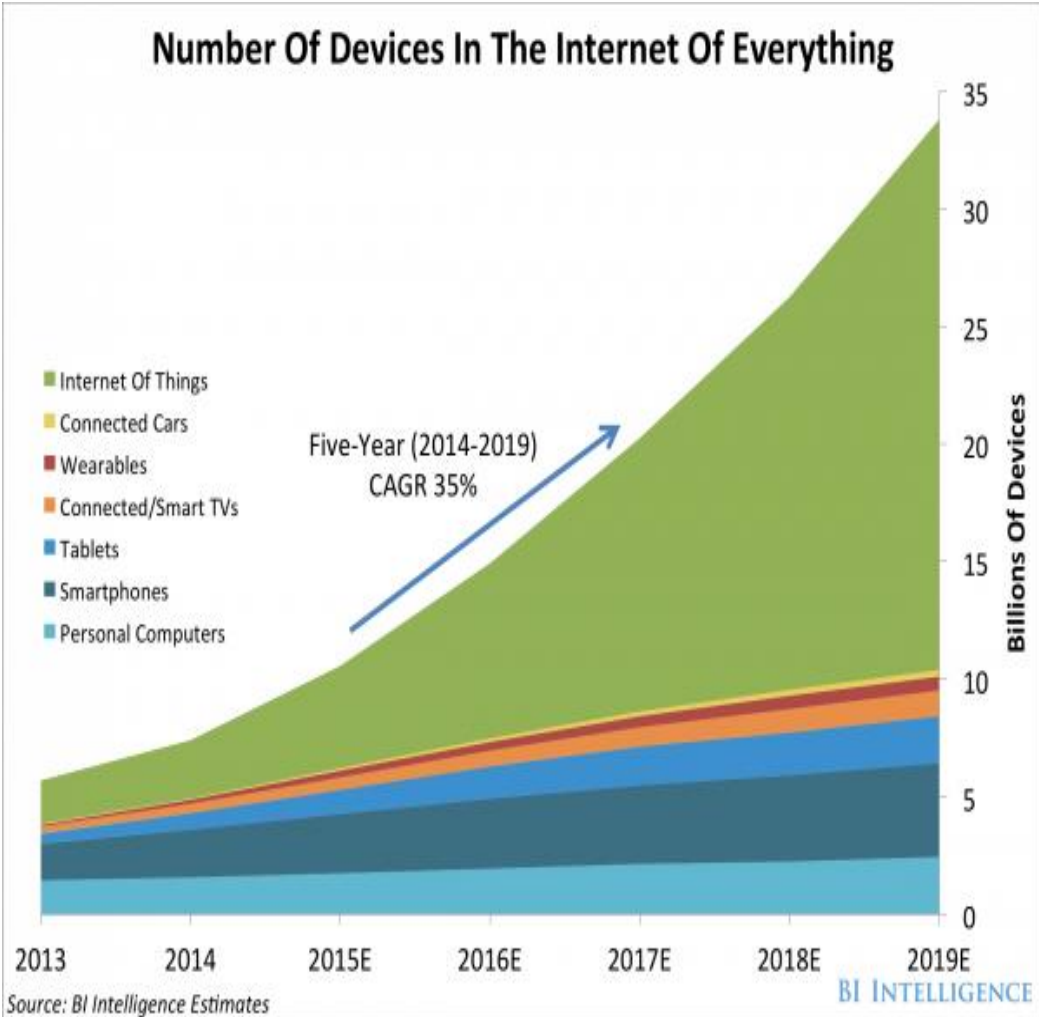


July 2019


❖ Outline

- Motivation
- Processor-Memory Wireless Interconnects in Metal Enclosures
- Channel Measurements in Metal Enclosures
- Channel Modeling of Propagation in Metal Enclosures
- Future Challenges

❖ Internet of Everything

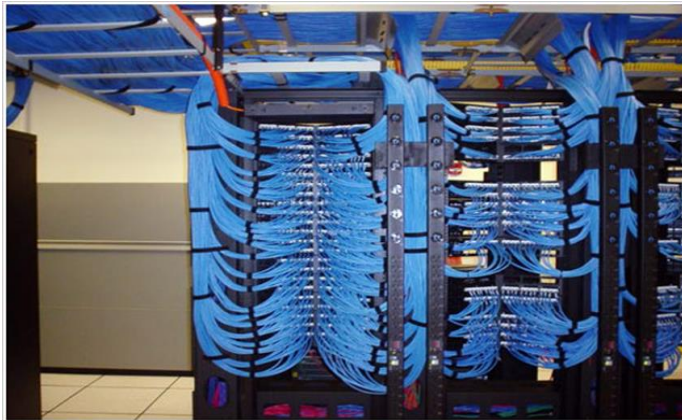


❖ Challenges for IoT and Wearable Devices

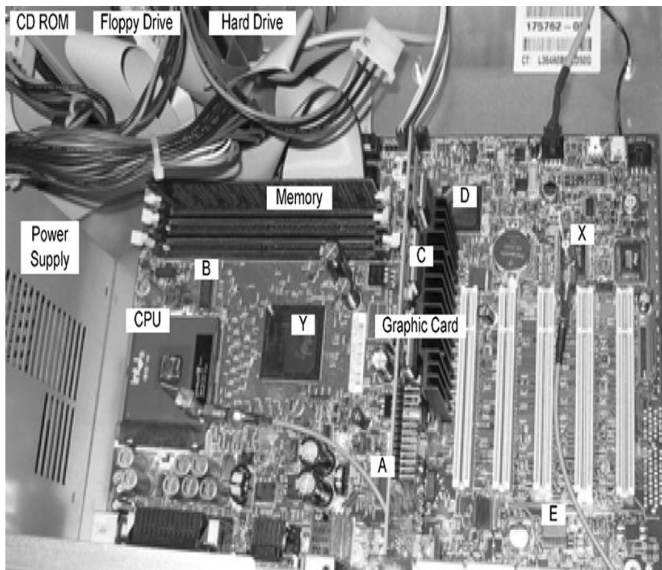
- **Sensing a complex environment** -Innovative ways to sense and deliver information from the physical world to the cloud
- **Connectivity-** Variety of wireless networks needed
- **Cloud is important** - IoT will require significant increase in data storage  needs better rack-to-rack, device-to-device, and chip-to-chip communication
- **Security is vital** - Detecting and blocking malicious activity
- **IoT is complex** IoT application development needs to be easy for all developers, not just to experts
- **Power is critical**

❖ Applications That Need THz Communication

Interconnects in Data Centers



Chip-to-Chip On Motherboard



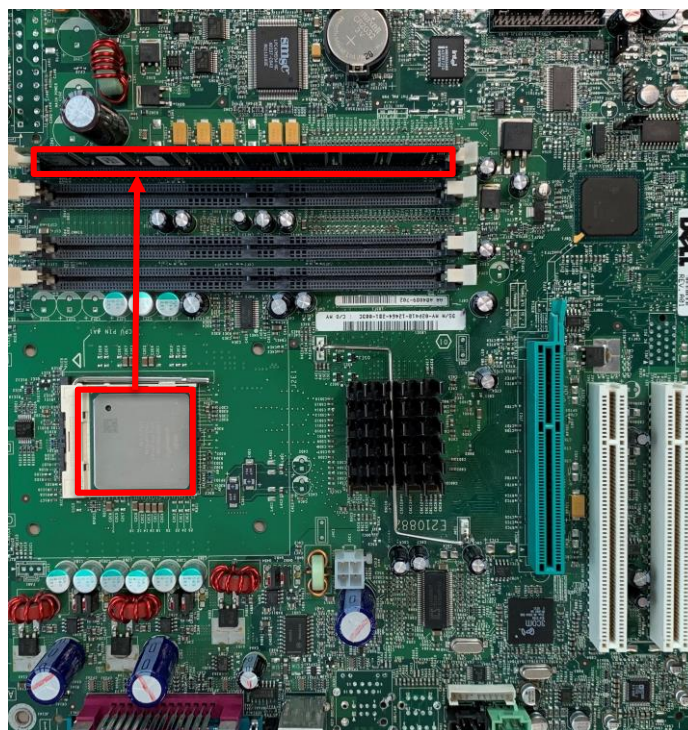
Wearable Devices



❖ Current Wireless Interconnects

- + antenna size/integration with chips
- +adding bandwidth without adding pins or fiber connectors to the chip package.
- - limited bandwidth
- For example, a computer in a typical high performance cluster gets 56 Gbits/s
- Wireless communication at mm- Wave frequencies: WiGig uses 60 GHz frequency range to provide up to 7 Gbits/s using OFDM, 64- QAM, and sophisticated coding.
- Power hungry systems

❖ THz Chip-to-Chip Wireless Communications in Metal Enclosures



- THz wireless communication on the motherboard, i.e. CPU-DIMM link, CPU-AGP link, etc.
- Channels are inside the desktop case which is mostly made out of metal.

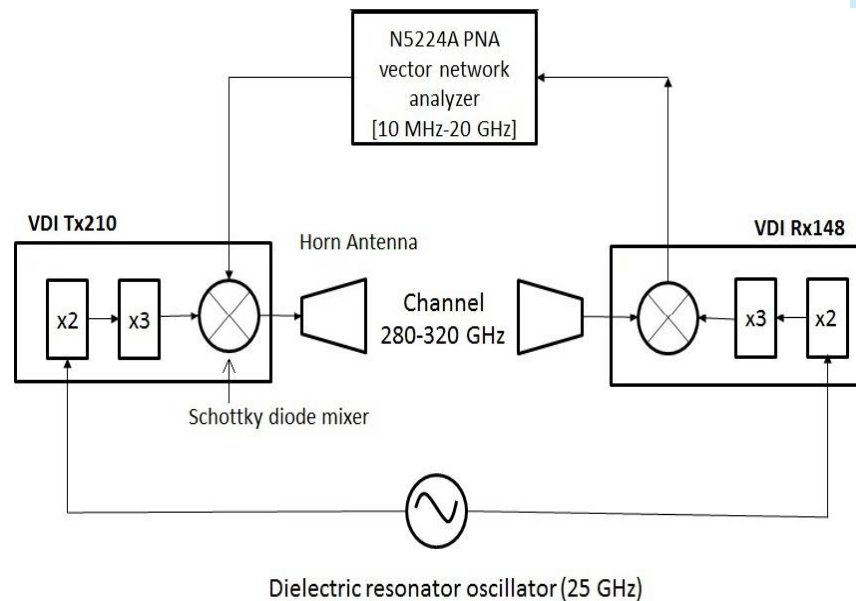
[1] J. Fu, P. Juyal, and A. Zajic, “300 ghz channel characterization of chip-to-chip communication in metal enclosure,” in 13th European Conference on Antennas and Propagation (EuCAP). IEEE, 2019, pp. 1–5.

❖ Measurement Setup

TABLE I
MEASUREMENT PARAMETERS

parameter	Symbol	Value
Measurement points	N	801
Intermediate frequency bandwidth	Δf_{IF}	20 kHz
Average noise floor	P_N	-90 dBm
Input signal power	P_{in}	0 dBm
Start frequency	f_{start}	10 MHz
Stop frequency	f_{stop}	12 GHz
Bandwidth	B	11.99 GHz
Time domain resolution	Δt	0.067 ns
Maximum excess delay	τ_m	40 ns

300-320 GHz Measurement System



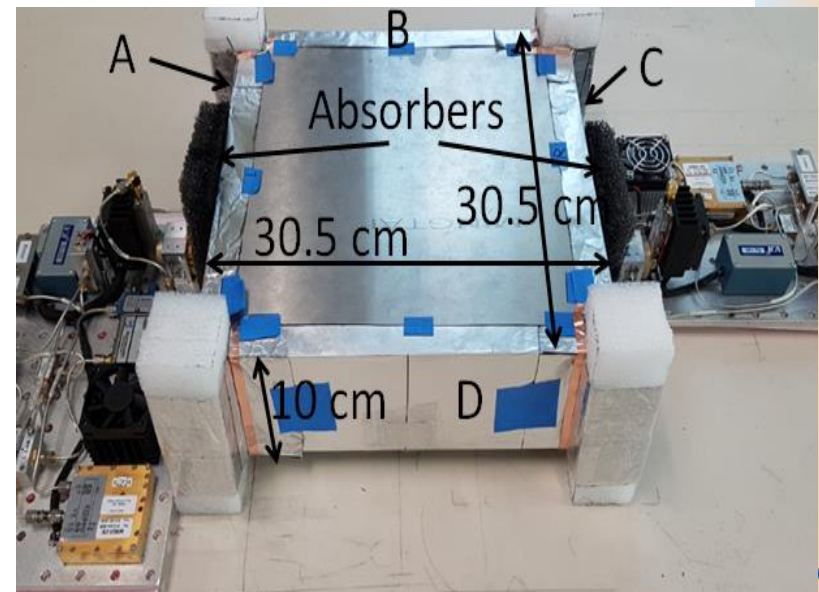
➤ THz Measurement Setup

➤ N5224 VNA

➤ Directional horn antennas with 3 dB beamwidths of 12° and the gain varies between 22 and 23 dBi.

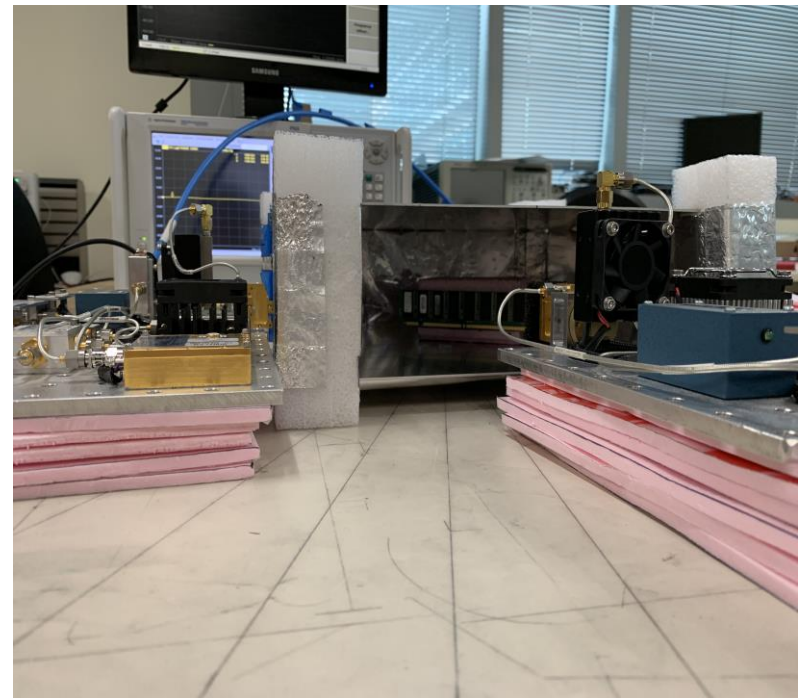
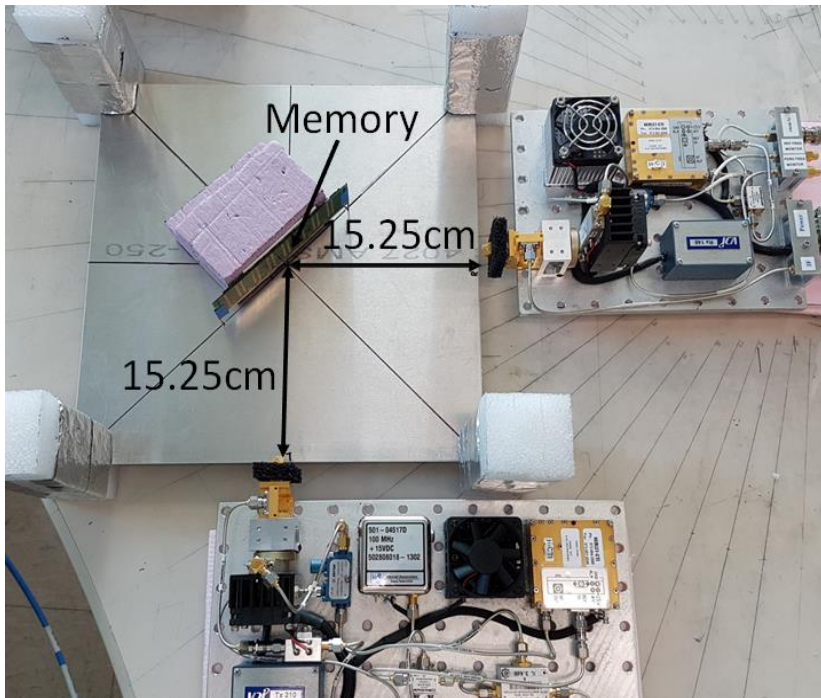
❖ Measurement Scenarios

- Line-of-sight inside a desktop size metal cavity
 - An aluminum cavity with the size of $30.5\text{ cm} \times 30.5\text{ cm} \times 10\text{ cm}$.
 - Cavity was in between the Tx and Rx with antennas aligned horizontally.
 - Transceivers' height, h , varied from 0 cm to 6.6 cm with the step size of 0.6 cm .
 - Absorbers were used to eliminate reflections from the backsides of antenna

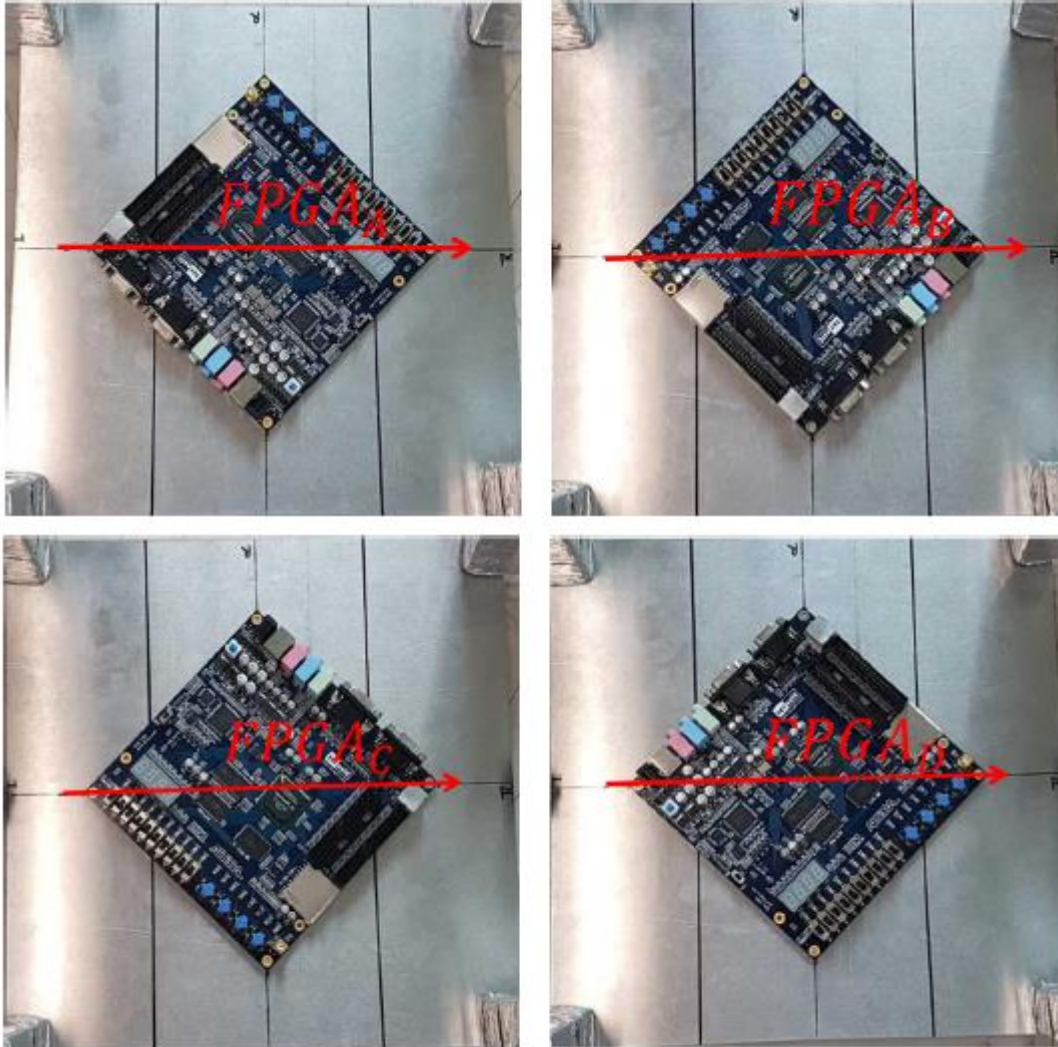


❖ Measurement Scenarios

- RNLoS with DIMM as the Reflecting Surface
 - Tx and Rx were positioned perpendicular with each other.
 - A dual in-line memory modules (DIMM) was vertically put on the center of the bottom of the cavity along its diagonal.
 - Both flat and component sides of the DIMM were measured.
 - Control experiments were performed in free space.

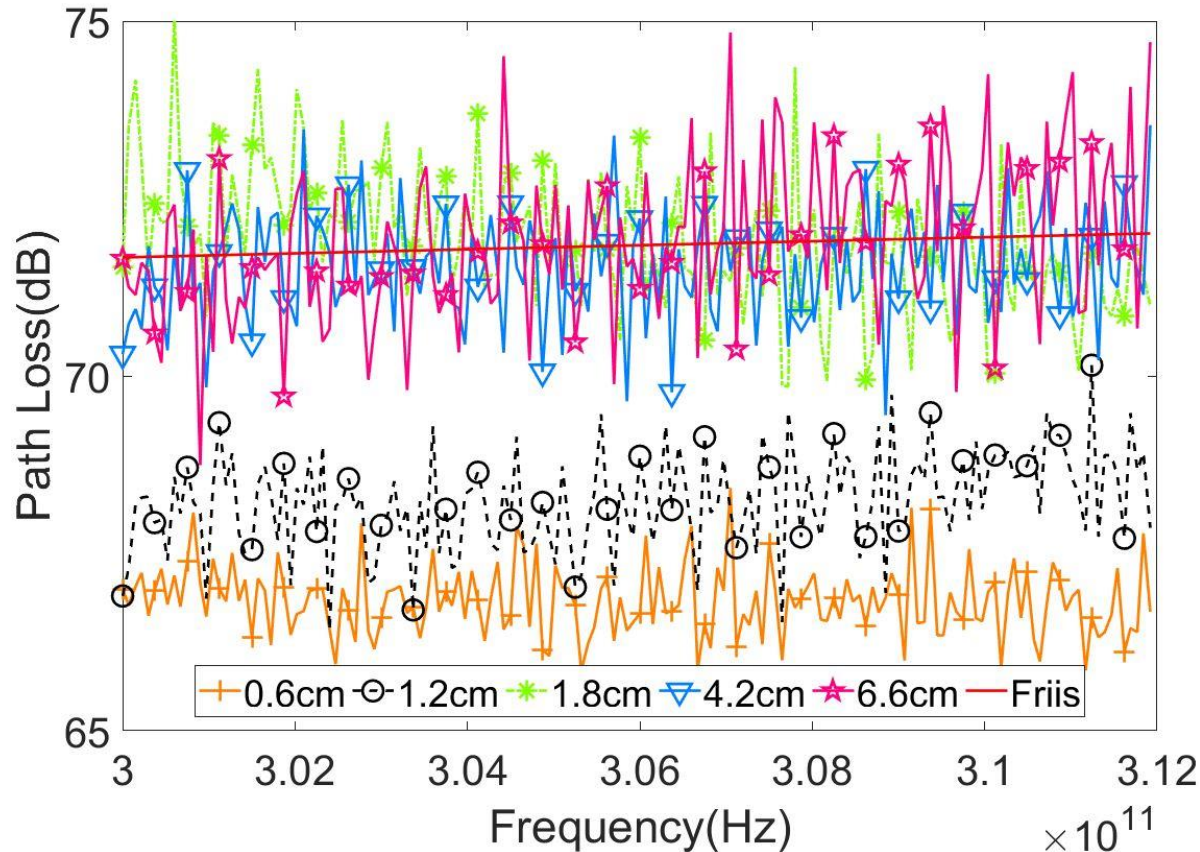


❖ Measurement Scenarios



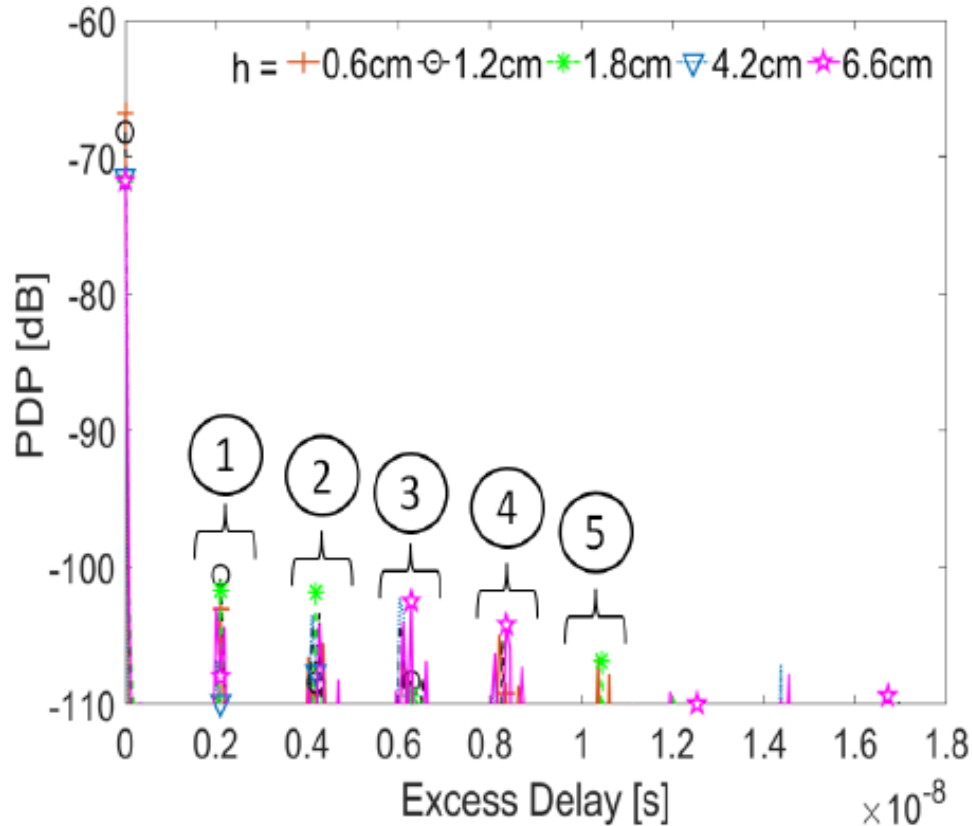
- LoS over FPGA board
- A FPGA board 15.2 x15.2 cm, the height of 1.5 cm.
- Located in the center of the bottom plate.
- EM wave travels through the FPGAs diagonals.
- Measured in air and in metal cavity

❖ Measured Path Loss Inside Metal Cavity



- For $h < 1.8$ cm, measured path losses are lower than the Friis prediction (ground reflection).
- For $1.8 \text{ cm} \leq h \leq 6.6$ cm, average of measured path losses are aligned with the Friis prediction.

❖ Power Delay Profile in Metal Cavity

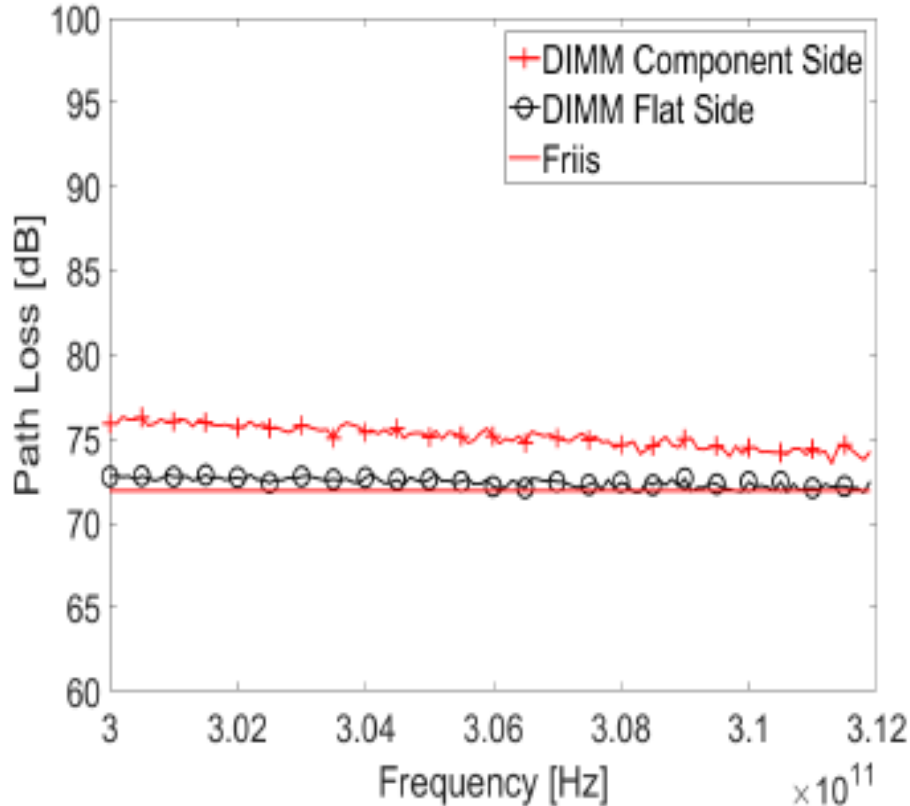


➤ Power delay profile

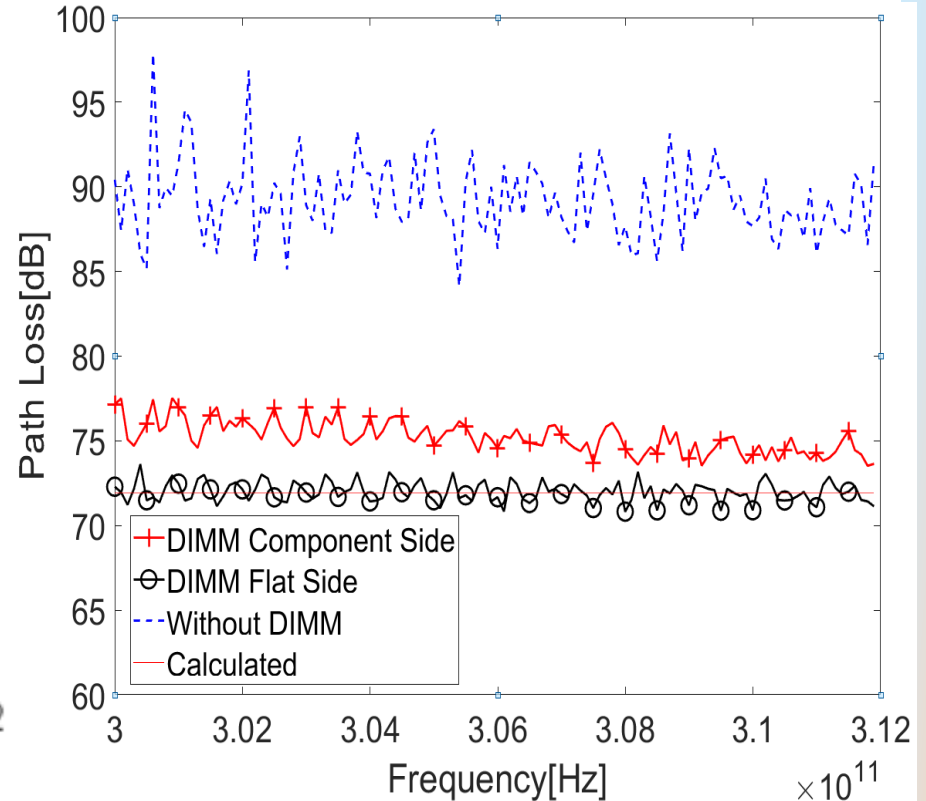
- There are several clusters of peaks that arrive with the delay of 2.05 ns.
- The difference between any two close paths is 61.5 cm (twice of the box's length).

❖ RNLoS Path Loss Inside a Metal Cavity vs. Free Space

➤ In Free Space

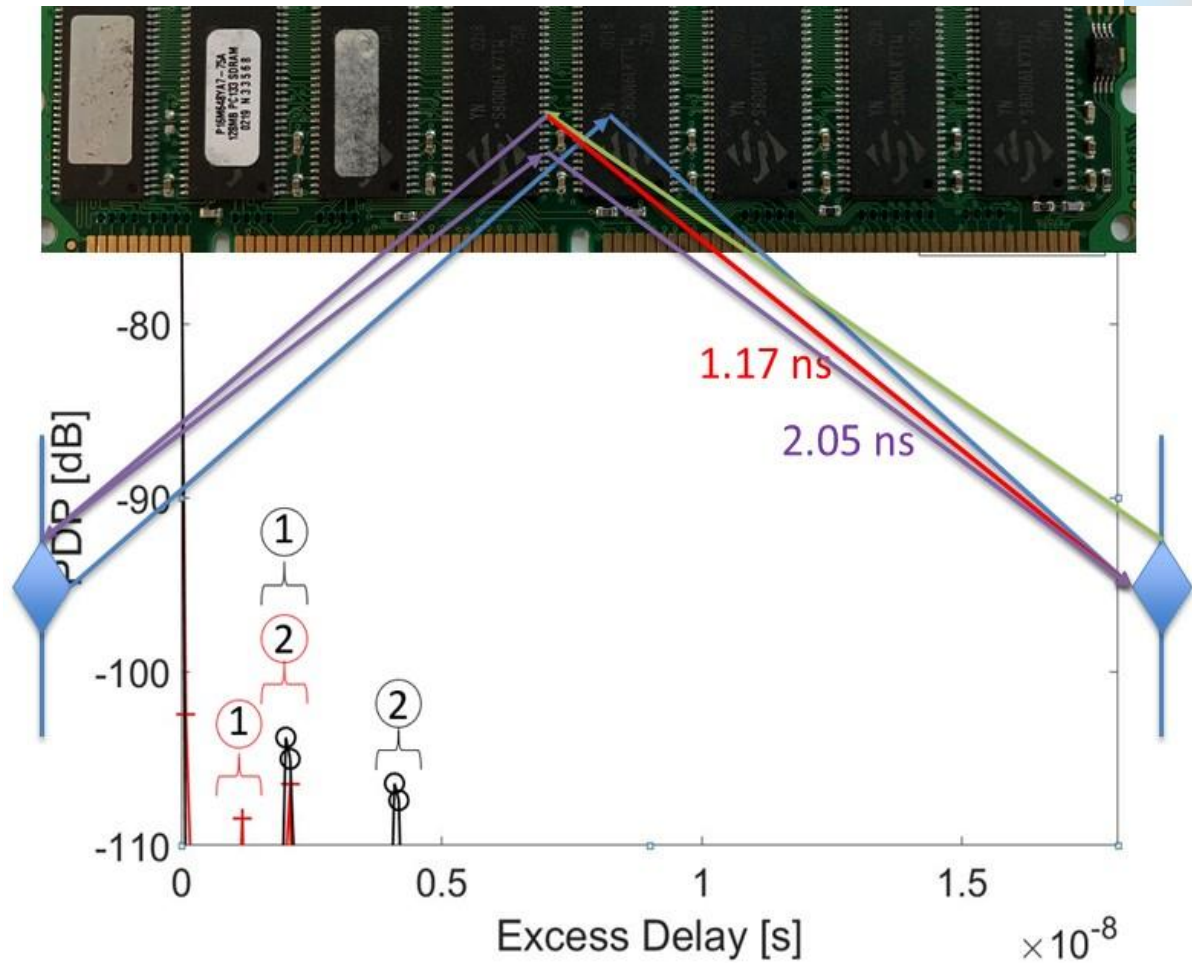


➤ In Metal Cavity



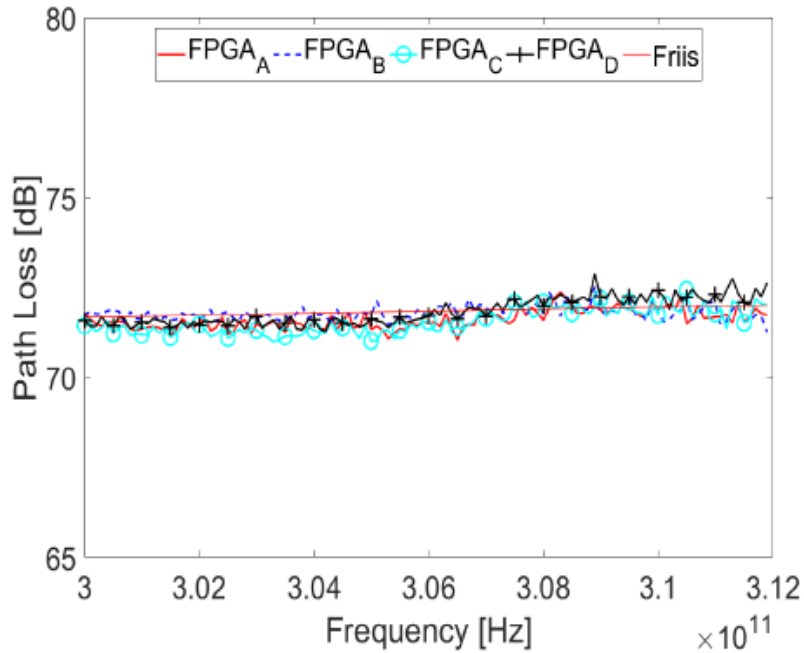
❖ RNLoS PDP Inside a Metal Cavity

- Power delay profile
 - Flat side of the DIMM
 - Two arriving peaks with excess delay of 2.05 ns and 4.09 ns.
 - Component side of the DIMM
 - Two arriving peaks with excess delay of 1.17 ns and 2.05 ns.

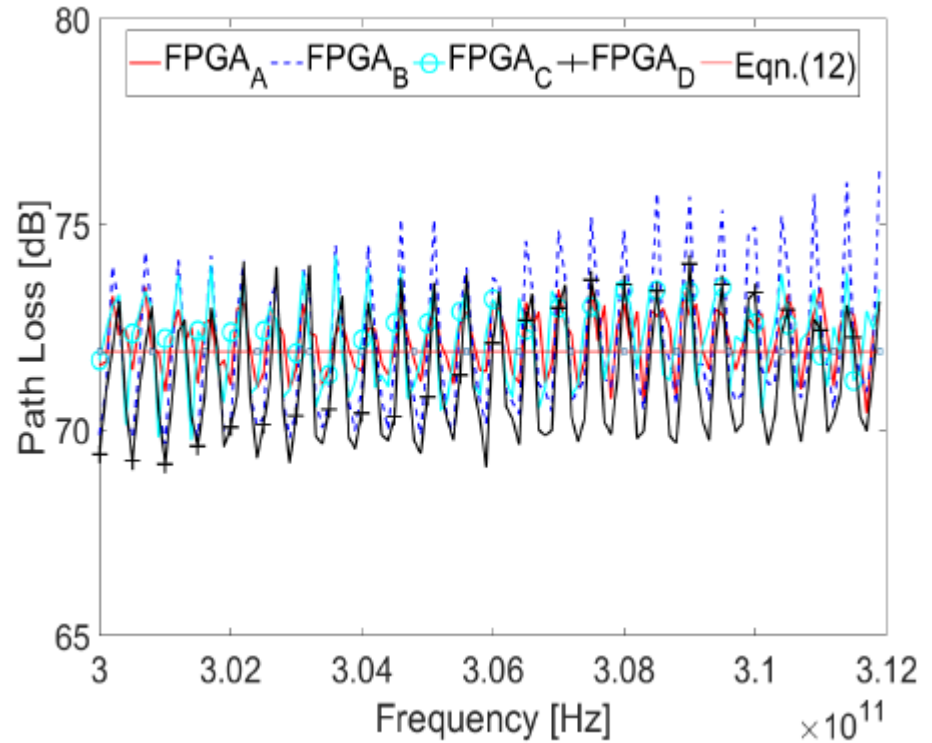


❖ RNLoS Path Loss Over FPGA

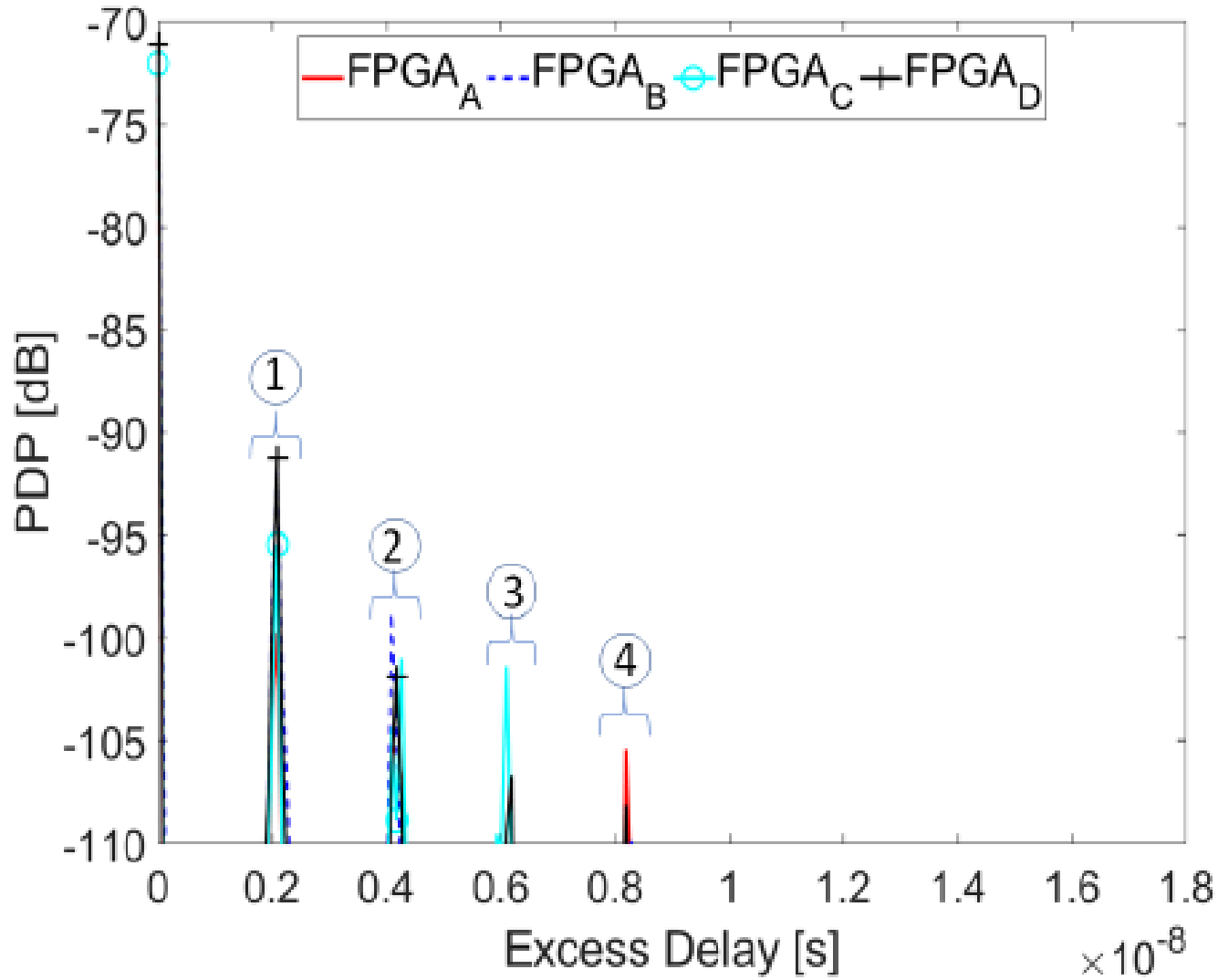
➤ In Free Space



➤ In Metal Cavity

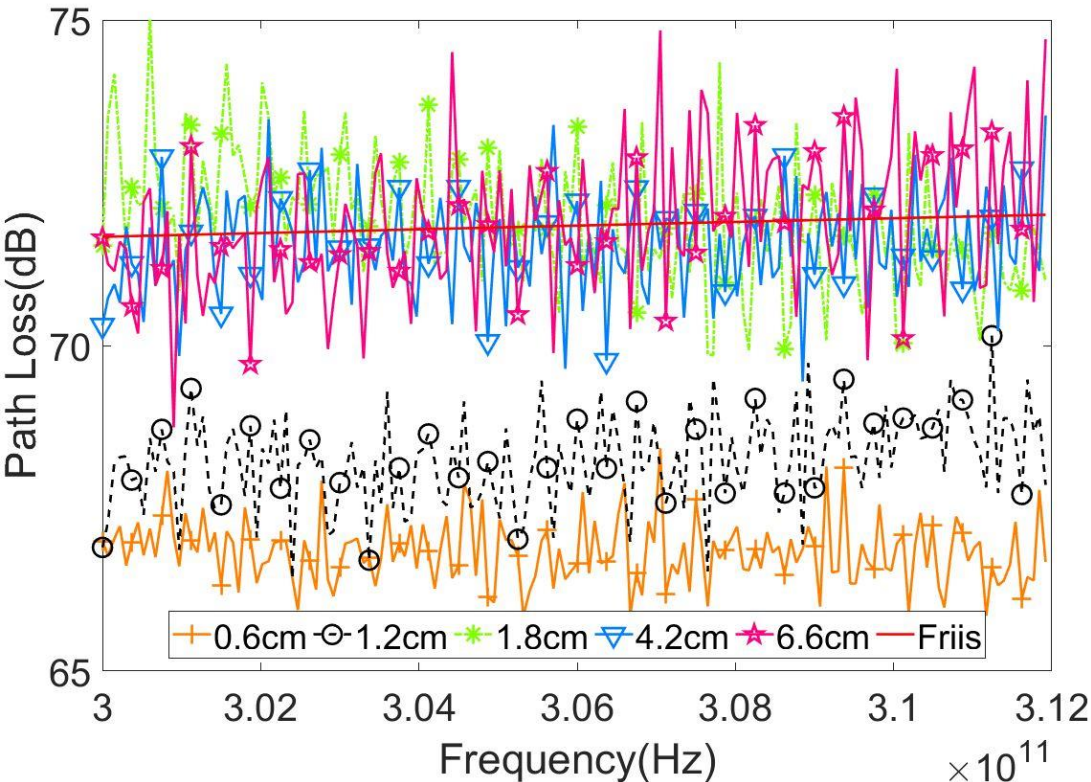


❖ RNLoS PDP Over FPGA



❖ Path Loss Model

$$(PL^T)_{dB} = \left(\overline{PL}\right)_{dB} + 10 \log_{10}(|E|^2)^{-1}$$



- $(PL^T)_{dB}$: theoretical path loss.
- \overline{PL} : mean path loss of traveling wave.
- $10 \log_{10}(|E|^2)^{-1}$: received power variation contributed by resonant modes

❖ Path Loss Model

$$(PL^T)_{dB} = \boxed{\overline{PL}}_{dB} + 10 \log_{10}(|E|^2)^{-1}$$

- Mean path loss
 - $\overline{PL} = \frac{1}{\Delta f} \int_{\Delta f} \left(\frac{4\pi df}{c} \right) df .$
 - $d = D = 30.5 \text{ cm}.$
 - c is the speed of light.
 - $\Delta f = 12 \text{ GHz}.$

❖ Path Loss Model

$$(PL^T)_{dB} = (\overline{PL})_{dB} + 10 \log_{10}(|E|^2)^{-1}$$

➤ Power contributed by resonant modes

➤ The transverse components of the electric field of TE mode.

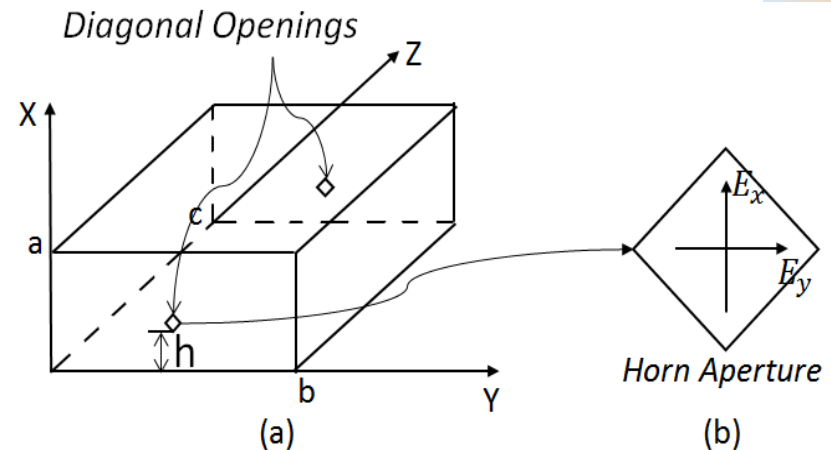
➤ $|E|^2 = |E_x|^2 + |E_y|^2$.

➤ $E_x = \frac{-j\omega_{mnp}\mu k_y H_0}{k_{mnp}^2 - k_z^2} \cos \frac{m\pi y}{a} \sin \frac{n\pi y}{b} \sin \frac{p\pi z}{c}$.

➤ $E_y = \frac{j\omega_{mnp}\mu k_x H_0}{k_{mnp}^2 - k_z^2} \sin \frac{m\pi x}{a} \cos \frac{n\pi y}{b} \sin \frac{p\pi z}{c}$.

➤ $k_{mnp}^2 = \left(\frac{m\pi}{a}\right)^2 + \left(\frac{n\pi}{b}\right)^2 + \left(\frac{p\pi}{c}\right)^2$.

➤ $f_{mnp} = \frac{1}{2\sqrt{\mu\epsilon}} \sqrt{\left(\frac{m}{a}\right)^2 + \left(\frac{n}{b}\right)^2 + \left(\frac{p}{c}\right)^2}$.

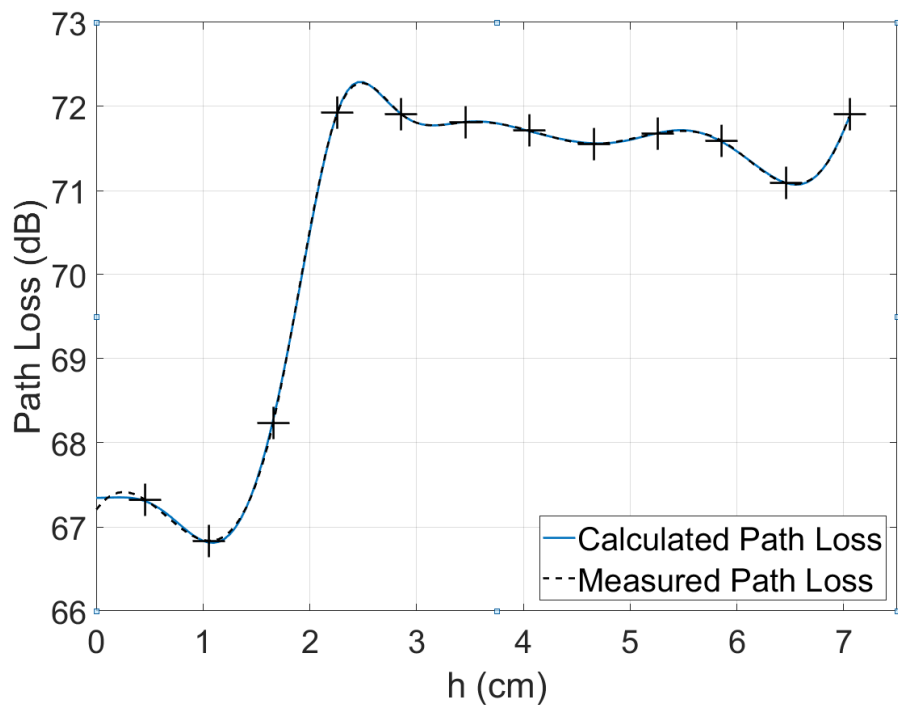


❖ Path Loss Model and Comparison With Measurements

➤ Resonate modes in the metal cavity

$$➤ E_x = B_m \cos \frac{m\pi x}{a}, E_y = A_m \sin \frac{m\pi x}{a}.$$

$$➤ |E|^2 = |E_x|^2 + |E_y|^2 = \left| \sum_{m=1}^M E_{xm} \right|^2 + \left| \sum_{m=1}^M E_{ym} \right|^2.$$



➤ The first 8 TE modes dominate the resonate modes inside the cavity with curve-fitting.

➤ The coefficients of these modes are

➤ $A_1 = 0.441,$

➤ $B_1 = -0.173,$

➤ $A_2 = -0.583,$

➤ $B_2 = 0.060,$

➤ $A_3 = 0.757,$

➤ $B_3 = -0.056,$

➤ $A_4 = -0.254,$

➤ $B_4 = 0.352,$

➤ $A_5 = 0.274,$

➤ $B_5 = -0.112,$

➤ $A_6 = 0.128,$

➤ $B_6 = 0.394,$

➤ $A_7 = 0.968,$

➤ $B_7 = 0.892,$

➤ $A_8 = 0.269,$

➤ $B_8 = 0.323.$

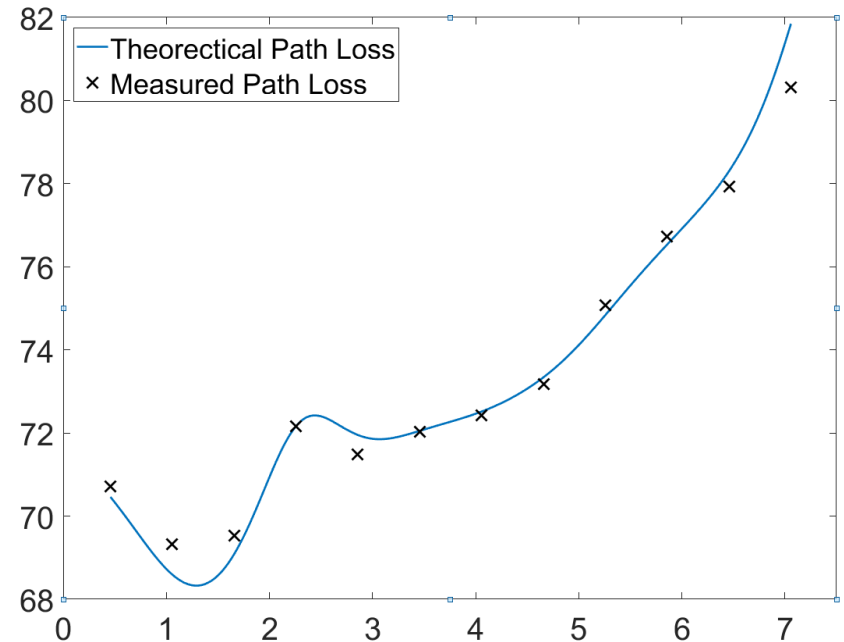
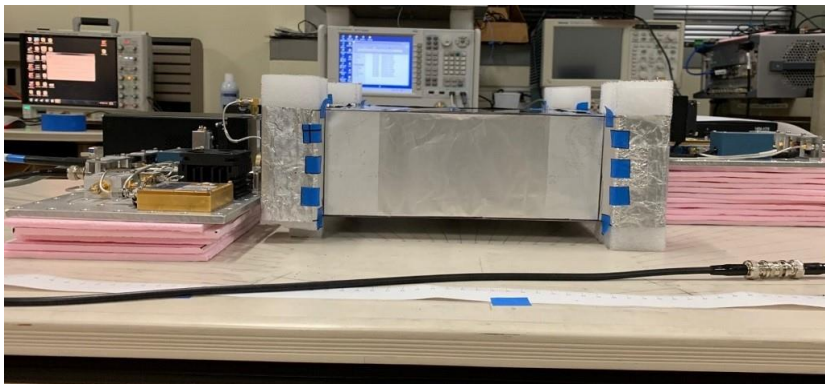
❖ Including Antenna Misalignment

$$(PL)_{dB} = \overline{(PL^t)}_{dB} + 10 \log_{10}(|E|^2)^{-1} + 10 \log_{10} \left(|g(\alpha_t)g(\alpha_r)|^2 \right)^{-1}.$$

- The loss due to the misalignment between the Tx and Rx.
- $g(\alpha)$ represents the radiation pattern of the diagonal horn antenna.
- $g(\alpha) = \begin{cases} X + Y \cos(Z\alpha) & -\theta \leq \alpha \leq \theta \\ c & \text{otherwise} \end{cases}$
- θ is half beamwidth of the diagonal horn antenna.

❖ Path Loss Model

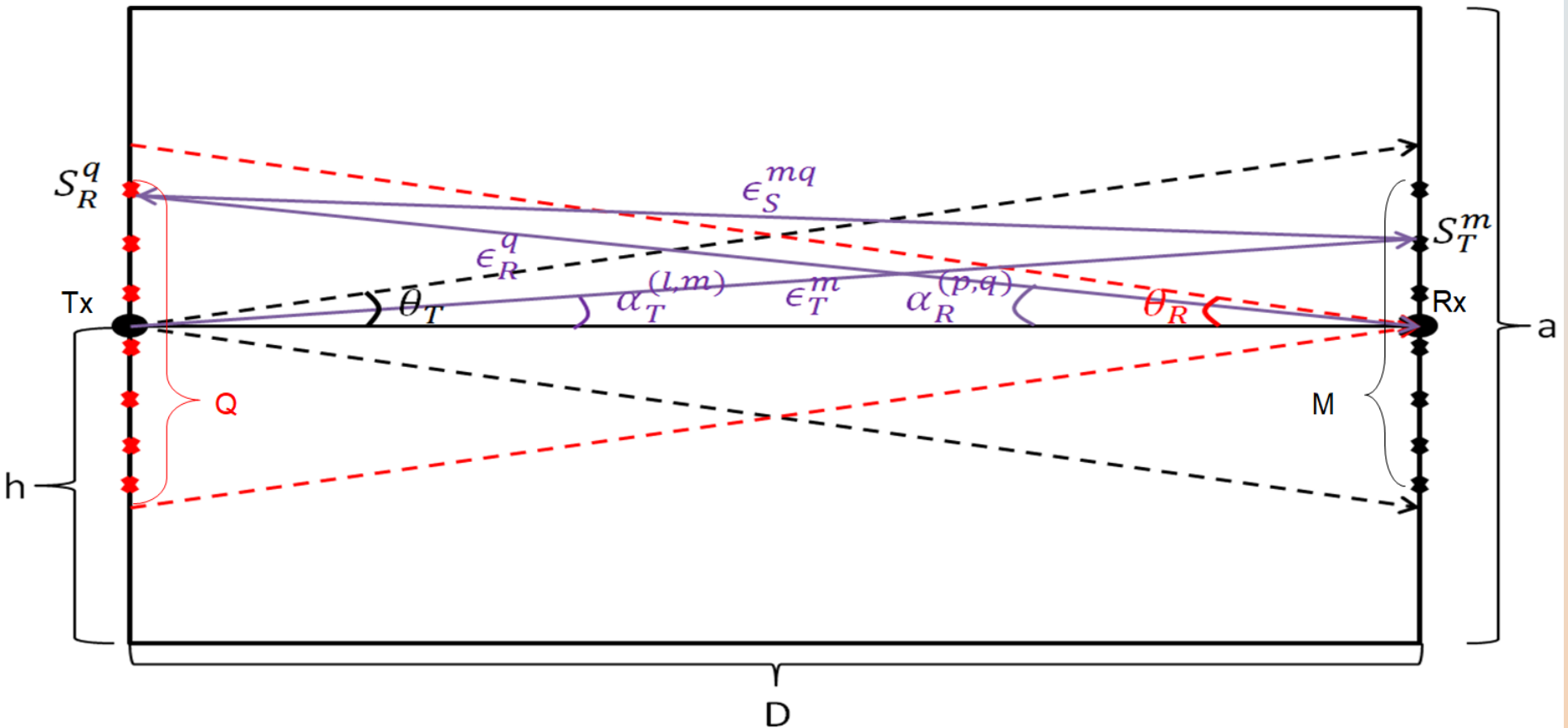
- Verification measurements
 - Similar measurement setup with the inbox LoS measurements.
 - Rx height, h_r , varies from 0cm to 6.6cm with Tx height, h_t , being fixed at 2.4cm .
 - A good agreement can be found between the measured and calculated path loss.



❖ Channel Modeling

- Both traveling wave and resonant modes exist inside the metal cavity.
- Traveling wave inside the metal enclosure is likely to excite the cavity.
- Transceiver sidewalls of the cavity can be treated both as consecutive scatters and the sources of EM waves.
- The generated EM waves are considered and modeled as multi-bounced (MB) rays.
- Two dominate propagation mechanisms:
 - LoS: signal travels directly from Tx to Rx.
- MB: signal bounces back and forth between the transceiver side

❖ Geometrical Model for LoS Propagation in Metal Cavity



❖ Model Parameters

- D, a: length and height of the cavity.
- h: height of both Tx and Rx.
- M, Q: scatters uniformly distributed on Tx and Rx sidewalls.
- θ_T, θ_R : half-beamwidth of Tx and Rx antenna.
- S_T^m, S_R^q : the m^{th} and q^{th} scatter on the Tx and Rx sidewall.
- α_T^m, α_R^q : the angle of departure and arrival.
- $\alpha_T^m = -\theta_T + \frac{2(m-1)}{M-1} \theta_T, \alpha_R^q = -\theta_R + \frac{2(q-1)}{Q-1} \theta_R$.
- $\epsilon_T^m, \epsilon_R^q, \epsilon_S^{mq}$: the distances of Tx - S_T^m, S_R^q - Rx, and S_T^m - S_R^q .

❖ Channel Model for LoS Propagation in Metal Cavity

- $h(\tau) = h^{LoS}(\tau) + h^{MB}(\tau).$
- $h^{LoS}(\tau) = \sqrt{\frac{K}{K+1}} A_{LoS} e^{j\phi_{LoS}} \delta(\tau - \tau_{LoS}).$
- K is the Ricean factor.
- A_{LoS} , $e^{j\phi_{LoS}}$, and τ_{LoS} represent LoS amplitude, phase, and time delay.
- $A_{LoS} = \sqrt{\frac{P_t G_t G_r}{PL_{LoS}}}$, where P_t , G_t , G_r , and PL represent transmit power, transmit gain, receive gain, and path loss.

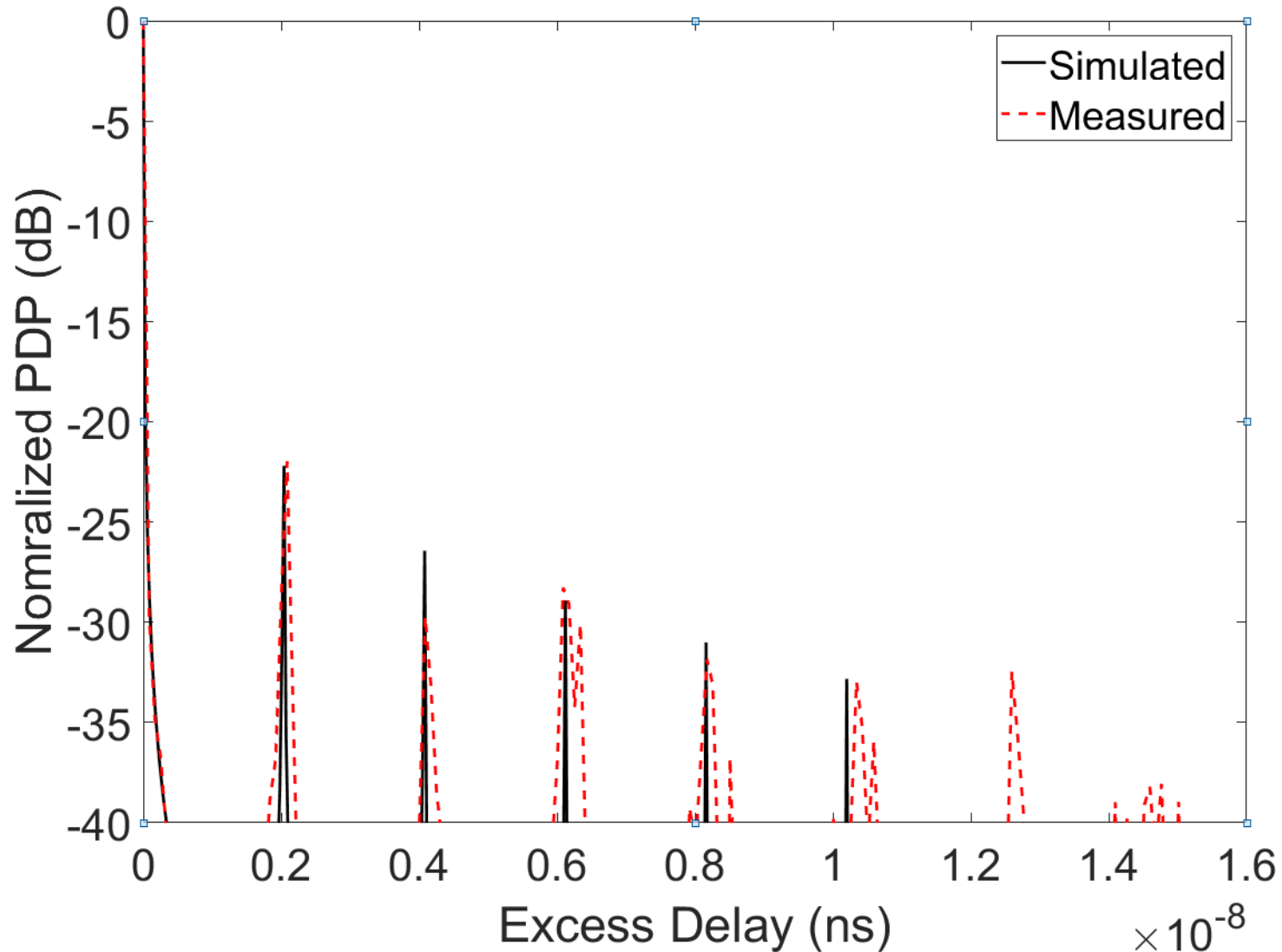
❖ Channel Model for LoS Propagation in Metal Cavity

- $$h^{MB}(\tau) = \sqrt{\frac{1}{K+1}} \cdot \frac{1}{\sqrt{LMQ}} \sum_{l=1}^L \sum_{m=1}^M \sum_{q=1}^Q A_{lmq} e^{j\phi_{lmq}} \delta(\tau - \tau_{lmq})$$
- L is the number of later arriving rays.
- A_{lmq} , ϕ_{lmq} , and τ_{lmq} represent the amplitude, phase, and time delay of multipath components.
- $$A_{lmq} = \sqrt{\frac{P_t G_t G_r}{P L_{lmq}}} f(\alpha_T^m) f(\alpha_R^q), \text{ where } f(\psi) = X + Y \cos(Z\psi).$$
- $$(PL)_{dB} = \left(\overline{PL} \right)_{dB} + 10 \log_{10} (|E|^2)^{-1}.$$
- $$\overline{PL} = \frac{1}{\Delta f} \int_{\Delta f} \left(\frac{4\pi d f}{c} \right)^2 df, |E|^2 = \left| \sum_{n=1}^N E_{yn} \right|^2 + \left| \sum_{n=1}^N E_{xn} \right|^2.$$
- For LoS: $d = D$.
- For MB: $d = D_L = \left(\epsilon_T^m + \epsilon_R^q + (2L - 1) \epsilon_{ang} \right), \epsilon_{avg} = \frac{1}{MQ} \sum_{m=1}^M \sum_{q=1}^Q \epsilon_S^{mq}.$

❖ Comparison Between Modeled and Measured PDPs

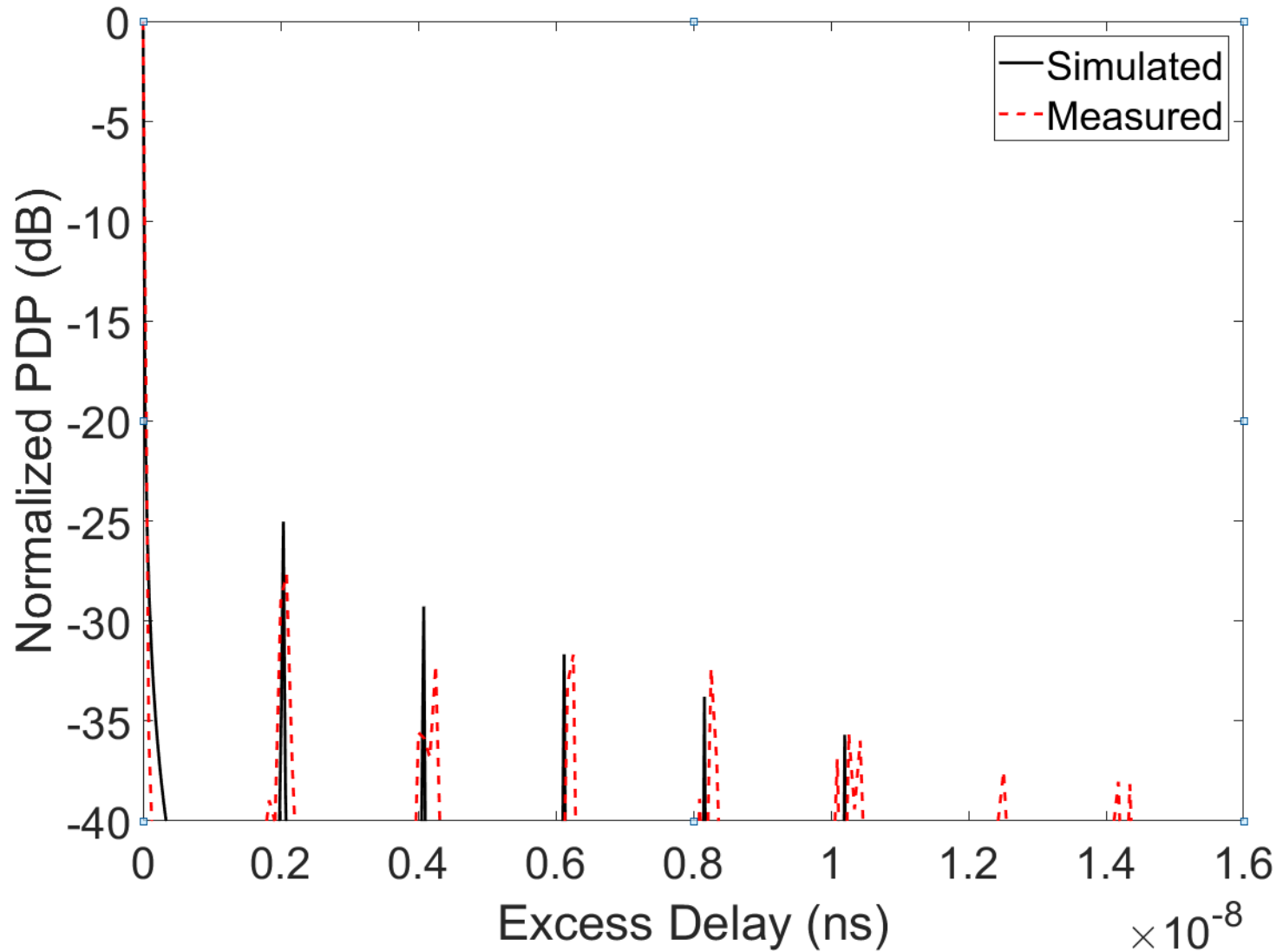
- The size of the metal cavity is 30.5 cm×30.5 cm×9.6 cm.
- The simulated PDPs are obtained with:
L=5, M=Q=45, K=17.36 and 33.04 for h=2.4 cm and 1.2 cm.
- Parameters for $f(\psi)$ are X=0.54, Y=0.45, Z=11.15.

❖ Comparison of Measured and Modeled PDPs



h=2.4 cm

❖ Comparison of Measured and Modeled PDPs



$h=1.2$ cm

❖ Summary

- Both traveling wave and resonate modes exist in the metal enclosure.
- The first 8 TE modes dominate the resonate modes in the metal cavity
- For the RNLoS propagation, traveling wave dominates channel.
- Also resonate modes lead to the stronger fluctuation of path losses over the frequency band.
- Statistical channel modeling can be used to represent resonant modes in the metal cavity

❖ Research Challenges

- Cost and energy efficient transceivers
- Antenna design for efficient communication over small distances
- Channel modeling at THz frequencies
- Low-complexity modulation and coding schemes



National Science
Foundation



THANK YOU

Questions?